STUDY ON ELECTROCHEMICAL BEHAVIOR COCRMO ALLOY USING EBM FABRICATED IN SIMULATED BODY FLUID

[1]YULI SETIYORINI, [2]SUNGGING PINTOWANTOROO, [3]YUICHIRO KOIZUMI, [4]KENTA YAMANAKA, [5]AKIHIKO CHIBA

[1]Graduate School of Engineering, Tohoku University, Sendai 980-8577, Japan
[2]Department of Materials and Metallurgical Engineering, Institut Teknology Sepuluh Nopember, Surabaya, Indonesia
[3]Division of Materials and Manuufacturing Science, Osaka University, Japan
[4]Institute for Materials Research, Tohoku University, Sendai 980-8577, Japan

Email: [1]yulisetiyorini@imr.tohoku.ac.jp, [2]sungging@mat-eng.its.ac.id, [3]ykoizumi@mat.eng.osaka-u.ac.jp, [4]k_yamanaka@imr.tohoku.ac.jp, [4]a.chiba@imr.tohoku.ac.jp,

Abstract: This study presents effect of direct build during EBM fabricated (0°, 45°, 55° and 90°) to the evolution of microstructure that influenced the properties of electrochemical involve passivity formation in blood plasma. The results was revealed during solidification of CoCrMo induce the precipitate formation in both grain boundaries and matrix grain. Precipitate was contributed to the range of passivity formation, due to induce the dissolution of metals in the electrolyte. However, the redox behavior was not influenced by microstructure and precipitate. It was only influenced by type of electrolyte composition. During contact with blood plasma, CoCrMo were performed oxide Cr_2O_3 and $Cr(OH)_3$, which high dominated by Cr_2O_3, respectively. From the bode phase and phase spectra were depicted of stability oxide formation whether in low frequency or high frequency. Impedance was described the nyquist spectrum with high semicircle perform in 55° of direct build both in Top part and Bottom part. In general, direct built parameter during EBM fabricated was give significant contribution to the stability of passivity formation due to the microstructure and precipitate distribution.

Index Terms: CoCrMo, Cyclic voltammetry, EBM (Electron Beam Melting), Impedance, Polarization.

INTRODUCTION

The excellent performance of CoCrMo has attract attention to use this alloys as medical devices particularly in hip and knee joints due to excellent corrosion and wear resistance [1]. Manufacturing technology is growing so fast. Recently, electron beam melting (EBM) has become popular and famous in additive manufacturing, due to the excellent advantages. It is to be high light, the ability to produce a complexes geometries that would not be able achieved using conventional manufacturing. This promises for metal implant production.
The preheating temperature causes transformation of metastable ɤ-fcc phase to ε-hcp phase[2]. The greater height of fabricated by EBM induces phase transformation at the bottom part which difficult to avoid due to long post-melting time. It resulted inhomogeneity of microstructure along the built height [3].

Some studies in clinical was reported that Cr detection in the blood[4]–[8]. It can occurs due to electrochemical reaction between metal and body fluids. This happened without any mechanically contribution such as wear. Cr debris from CoCrMo will bound to components with low molecular weight thus leading to hemoglobin directly[6], [9]–[11]. It gives betterexplanationabout difficulty to detach chromium in the urine from individuals has expose of Cr[8], [9].
Electrochemical studies can be used to understanding of biocompatibility CoCrMo due to the passivity formation. It known that passivity related to the corrosion resistance of alloy. The stability of passivity formation becomes important to protect the surface of alloy during contact with body fluid, include blood. Blood plasma is part of blood that contain a lot of ions that suggested contribute to the electrochemical reaction due to contact with metal alloys.
In this study, the effect of direct built during fabricated will investigatethe electrochemical behavior due to contact to the blood plasma.

EXPERIMENTAL

The geometry of rod CoCrMo alloy that fabricated using EBM is 16 mm in diameter and 160 mm in height. Four direct build were applied in EBM fabrication process involve 0°, 45°, 55° and 90°. The CoCrMo alloys was cut in 1 mm of thickness from the rod and distinguished between top and bottom part. Top and bottom part were took 5 mm from the edge. All were wet ground with silica paper until 2400 grid, further continued with OPU. Furthermore, it was cleaned with ethanol in ultrasonic bath. Simulated Body Fluid (SBF) was used in all experiment by using Kokubo c-SBF [12].
The EBSD investigation was performed using field emission SEM (FESEM) (FEI XL30S-FEG) with operate at 15kV. Meanwhile, observation of SEM was employed using SEM (FESEM) (Carl Zeiss ULTRA 55) at acceleration voltage 15kV, respectively. The composition of the CoCrMo alloys was revealed in Tabel 1.

Table.1 Chemical composition of CoCrMo alloys both Cast Forging and EBM fabricated

Elements	Wt.%
Co	Bal.
Cr	28.40
Mo	6.66
Ni	0.18
Si	0.45
Mn	0.69
C	0.23
N	0.20
O	0.023

The potentiodynamic polarization and cyclic voltammetry test were performed by scanning the applied potential from -1.5 V and moved 1.5 V at the scan rate of 10 mV/s. The software analysis was used CS Studio 5. Counter electrode was used carbon rods. Saturated calomel electrode (SCE) was employed as reference electrode. EIS measurement was carried out under potentiodynamic conditions in range applied potential from -1.5 V to 1.5 V. Impedance was performed for 10 frequency decades from 10^0 Hz to 10^5 Hz with an amplitude of ± 10 mV and scan rate of 10 mV/s. The data was analyzed using Zview software. A double wall three-electrode cell of Teflon was used for all experiment.

RESULTS AND DISCUSSION

1.1. Microstructures and constituent phase

The EBSD analysis was conducted only focusing on the ɤ-fcc and ε-hcp matrix phases. From Figure 1, Cast Forging was revealed combination of phase. It was contained ɤ-fcc with small ofε-hcp that distributed in the matrix. The effect of direct build was significant clear. Along the height at 160mm, the top part was dominated by ɤ-fcc, meanwhile the bottom part was dominated with ε-hcp. Even in 55 Bottom, the bottom part was mix between ɤ-fccand ε-hcp with higher ratio of ε-hcp. Direct build 90° was resulted height as the diameter (16 mm), it indicated that phase both in top and bottom part was dominated by ɤ-fcc. The evolution of microstructure along vertical axis can be explained by relationship between the phase transition temperature and the temperature of the CoCrMo alloy during EBM fabrication.

Takashima et al. reported that during cooling process the section closer to the bottom part was held at high temperature for long period. It was induced for the transformation of ɤ to ε. Furthermore, the bottom part was dominated by ε phase. In other hand, the ɤ phase was become high in the top part. In addition, the prediction of ε phase would occurred at a height of 80 mm during fabrication [13]. This also confirmed by Shun et al. investigation. It was strong correlation between ɤ phase and ε phase due to martensitic transformation which maintained the Shoji-Nishiyama orientation relationship [14].

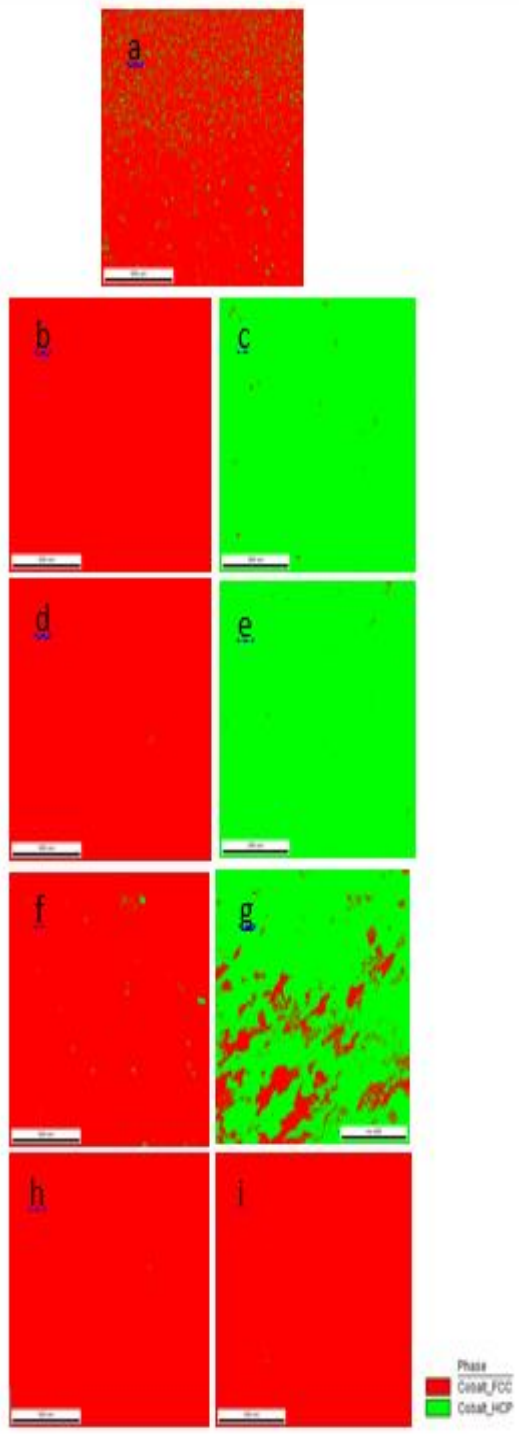


Figure 1: EBSD phase maps of CoCrMo alloys with different direct building and position along vertical: a. Cast Forging, b. 0 Top, c. 0 Bottom, d. 45 Top, e. 45 Bottom, f. 55 Top, g. 55 Bottom, h. 90 Top, i. 90 Bottom

Figure 2 was shown the grain boundary (GB) maps. The black, green and red lines was indicated theangle boundaries with misorientation (2°<θ<5°), (5°<θ<15) and (15°<θ<180). All CoCrMo alloys were identified with high angle grain boundaries (dominated with blue). Exceptional was occurred in 0 Top, it indicated combination between (5°<θ<15) and (15°<θ<180). The grains were dominated by high angle grain boundaries.

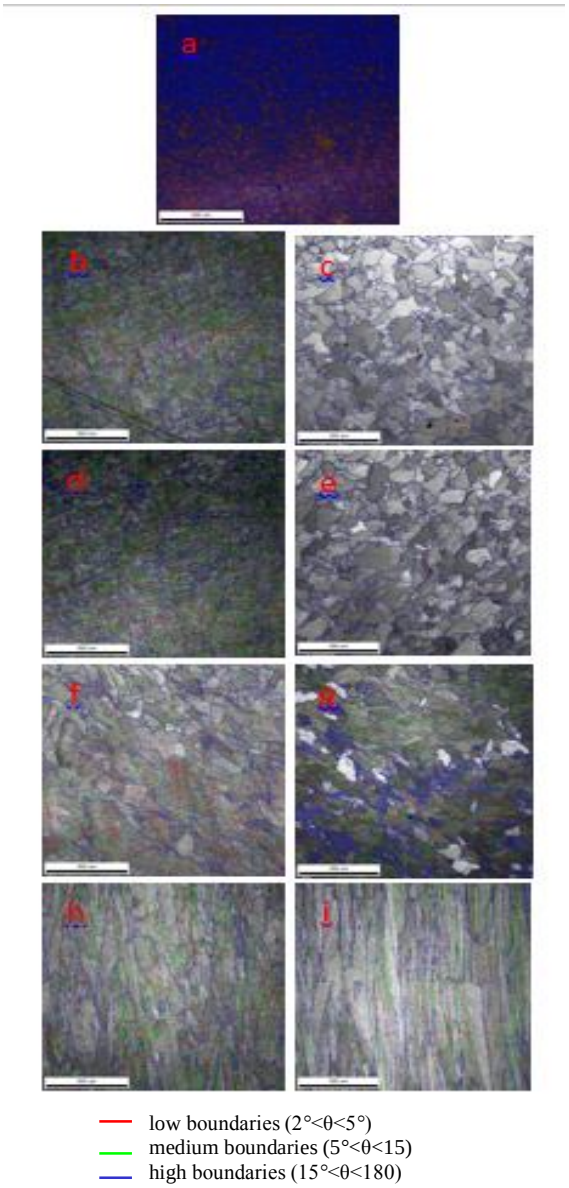


Figure 2: Grain Boundaries images of CoCrMo alloyswith different direct building and position along vertical: a. Cast Forging, b. 0 Top, c. 0 Bottom, d. 45 Top, e. 45 Bottom, f. 55 Top, g. 55 Bottom, h. 90 Top, i. 90 Bottom

Production of carbides is from saturated carbon level in the solid stage. The growing of the carbides is controlled by metal atom diffusion from the surface to carbides structure. The size and composition due to the cooling rate during solidification [15]–[17]. Formation of carbides was caused irregularities and heterogeneities in the adjacent zone (surrounding grain boundaries). It will contribute in the alloys dissolution. Several of distribution precipitate was depicted in Figure 3. A small number of black precipitate were noticed in all CoCrMo. Fine precipitate was observed in range several tens to a few hundred nanometer in diameter. Precipitate was distributed not only in the grain boundaries but also in the matrix grain.

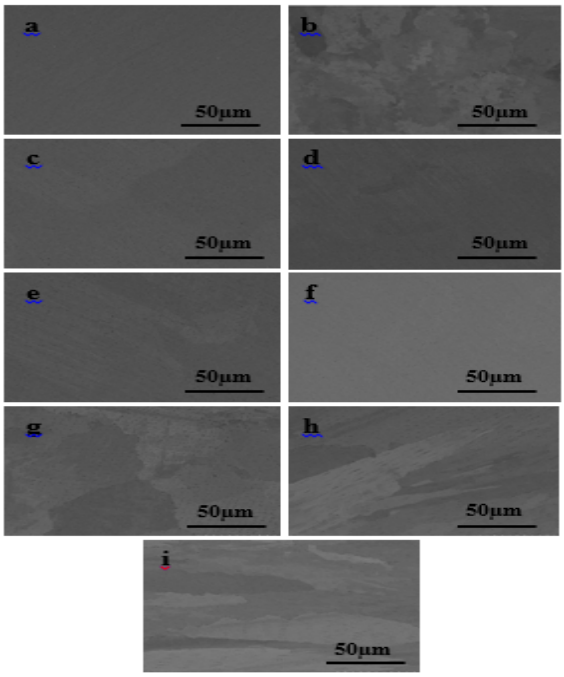


Figure 3: SEM-BSE images of CoCrMo alloyswith different direct building and position along vertical: a. Cast Forging, b. 0 Top, c. 0 Bottom, d. 45 Top, e. 45 Bottom, f. 55 Top, g. 55 Bottom, h. 90 Top, i. 90 Bottom

The polarization curves of CoCrMo alloys in SBF condition was depicted in Figure 4. All are divided in four potential domains. First, the cathodic region was started at -2.5 V until corrosion potential (E_{corr}) which indicate the reduction of water partially oxygen dissolved (called hydrogen evolution). The second region was performed the transition from cathodic to anodic current (called E_{corr}). In the next region was recognized to the passive area which indicate no change in current density. In the transpassive region was performed increaseof current due to chromium oxide dissolve then continuing to oxygen evolution. However, during transpassive domain was performed secondary passivity(shoulder phenomenon) that indicate the solubility of Co interact with electrolyte to produce $Co(OH)_2$ (0.54 V-0.64 V).In addition, it was reported that shoulder phenomenon was attributed to contribution of formation Co phosphate and Co carbonate (phosphate ion complexes)[18]–[20].

In the SBF at pH 7.4,from Figure 4 was exhibited active/passive behavior in all CoCrMo alloys. The E_{corr} of CoCrMo alloys were performed at ~(-0.9) V to (-0.4) V with quick to transform in passivity start at ~(-0.5) V to ~(-0.4) V and finish at ~0.2 V.The E_{corr} of 0 Bottom and 45 Top were shown more anodic compare than others. However, both of them just performed shorter range of passivity region. It suggested due to the carbide formation in the microstructure.It was reported by Bertini et al. that passive dissolution of alloys dominated occur in carbide boundaries zone [21], [22].Due to c-Kokubo SBF contain phosphate, it was suggested that it will

contribute to the production of hydrogen phosphate ions [19]. It became constitute a conjugate base of phosphoric acid. Asthe result, a weak acid may increase dissolution of CoCrMo [23].

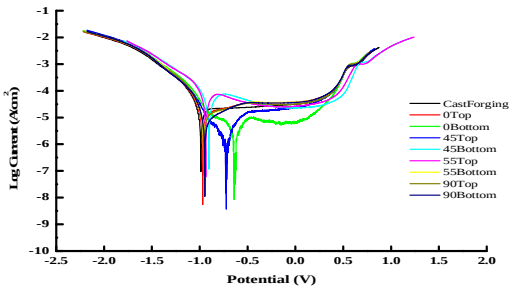


Figure 4: Polarization curve of CoCrMo alloys in SBF

The electrochemical behavior of CoCrMo in SBF (artificial blood plasma) was characterized by the cyclic voltammetry presented in Figure 5. It was performed similar trend in all CoCrMo alloys. There are three distinct regions in the potential range (-1.5 V-1.5 V) determined: the hydrogen evolution, the oxide film region and transpassive region followed by the oxygen evolution. In the oxidation, the first passivity region was observed in potential range -1.2 V to 0.5 V, then following with a peak as secondary passivity. This phenomenon oxidation was suggested as $Co(OH)_2$[24], while in reduction it proceed non-detectable amount of Co[25].The reversible potential corresponding to the reaction bellow, which it *vs* SCE reference [26].

$$Co + 2OH^- \leftrightarrow Co(OH)_2 + 2e \quad E°(V) = 0.73 \quad \ldots\ldots(1)$$

During the reduction, after transpassive the curve backward to form a peak reduction in potential -1.48 V. The reduction peak was observed of $Cr(OH)_3$ reduction due to the half-reaction *vs* SCE reference[26]:

$$Cr(OH)_3 + 3e \leftrightarrow Cr + 3OH^- E°(V) = -1.48 \quad \ldots\ldots\ldots(2)$$

Manufacturing technology of CoCrMo was not influenced the behavior of oxidation and reduction during electrochemical in SBF. Cast Forging and EBM in various direct build have the same trend.

The FTIR peaks of surface CoCrMo alloys after cyclic voltammetry was shown in Figure 6. From here, the different of oxide formation significant clear. Cr_2O_3 wasdominated as oxide in CoCrMo alloys after contact with SBF. Meanwhile, $Cr(OH)_3$ was found with not strong transmittance intensity. During contact with SBF was induced formation of Cr_2O_3 and $Cr(OH)_3$ in all CoCrMo alloys.

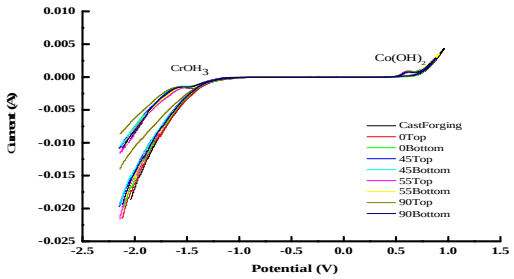


Figure 5: Voltammogram curve of CoCrMo alloys in SBF

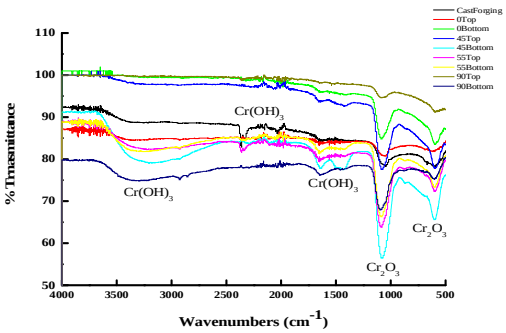


Figure 6: FTIR peaks of CoCrMo alloys in SBF

The impedance spectroscopy result of CoCrMo alloys in SBF at selected potential values was presented as Bode diagrams (Figure 7). All CoCrMo alloys were exhibited higher impedance in over the entire frequency range. The higher the impedance in high-frequency region suggested the better ability to mitigate charge transfer process, however the higher impedance in low-frequency region indicates better resistance to mass transport[27]. At high frequencies (10^3 to 10^5) the absolute impedance curve is almost independent of the frequency. This represents the electrolyte resistance. However, the electrolyte resistance in pH 7.4 was performed from 10^3-10^4, then followed by enhance the absolute impedance. Only 0 Bottom was performed increase the absolute impedance dependent of the frequency.

From the phase spectra, it is possible to predict the presence of a compact passive film if the phase angle is closed to 90° over a wide frequency range and if the spectrum shows linier portion at intermediate frequency [28]. Due to frequency range of phase angle higher than 70°, it suggested thecharge transfer process has been retarded[29]. It is attributed to the presence of oxide or amorphous surface layer that is free from defect of dislocation or grain boundaries. It is known that dislocations or grain boundaries can enhance ionic transport [30].

Figure 8 was depicted phase spectra of CoCrMo, which indicate the formation of passivity. All CoCrMo alloys was exhibited trend higher impedance in 10^2 frequency, except 0 Bottom.Then, it was decreased at 10^0 frequency. The 55 Top was performed the stable of passivity until low frequency which indicate a plateau line. O Bottom was performed differently, the phase spectra was achieve 80° at high frequency, which indicate the passivity was occurred in high frequency. However, the passivity formation was not stable, it drawback at 30° at low frequency. It noticed from our previous research that 0 Bottom was dominated by hcp (ε) in their microstructure [14]. Further, it was caused the electrolyte resistance raise in high frequency due to the retardation of in charge transfer.

It suggested oxide chromium formation in the inner is strong contribution. This data correlate to the peaks FTIR, that 0 Bottom was dominated by Cr_2O_3

through high transmittance intensity. Unfortunately, this oxide is less stable in low frequency due to the passive dissolution of ion metal (oxide film ruptured) during electrochemical. In SBF pH 7.4, most all CoCrMo was performed drop of phase in the lower frequency. Decrease the phase indicate that the dissolution ion metal is higher.

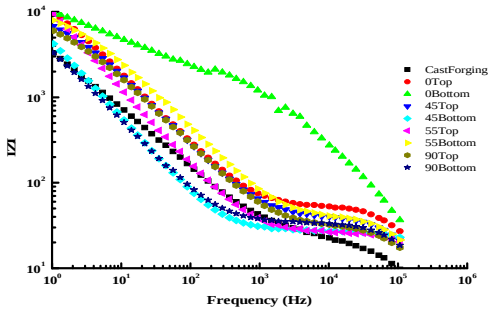


Figure 7: Bode spectrum curve of CoCrMo alloys in SBF

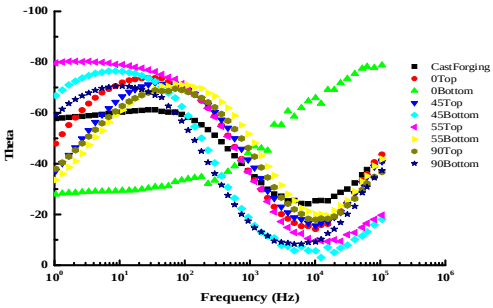


Figure 8: Phase spectra of CoCrMo alloys in SBF

From the nyquist spectrum, generally a larger capacitive loop corresponds to better corrosion resistance. In addition, the appropriate film thickness and fewer defects results in the best corrosion resistance of CoCrMo alloy. According to the nyquist plot (Figure 9), all CoCrMo were performed two semicircle. First semicircle was indicated by oxide film formation on the surface. Further, the next semicircle was performed by increasing the impedance imaginer due to increasing the real impedance, which indicate mass transfer occurred.

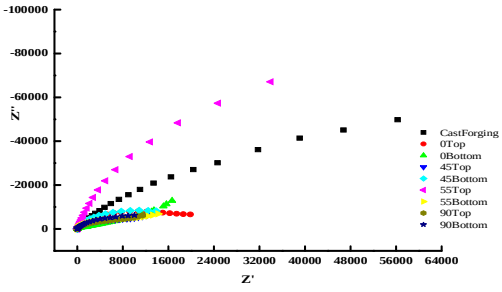


Figure 9: Nyquist spectrum of CoCrMo alloys in SBF

It suggested that this phenomenon correlate with passive dissolution then followed with transpassive behavior. The effect of build direction and position along vertical was significant different in nyquist results. The 55 Top was indicated of better corrosion resistance, the following with Cast Forging. It suggested that the effect of precipitate on the structure was influenced the passivity ability.

CONCLUSION

Technology manufacturing gives a great impact to the microstructure development of CoCrMo alloys. Investigation of electrochemical was given a better understand to the passivity formation during contact to blood plasma. Passivity was significant influenced by microstructure and precipitate distribution. In order to investigate the better performance of CoCrMo alloys in blood plasma, 55° of direct build was performed better passivity in blood plasma both Top part and Bottom part.

ACKNOWLEDGEMENTS

This study was supported by grant Hitachi scholarship period 2016-2019.

REFERENCES

[1] A. Chiba, K. Kumagi, N. Nomura, and S. Miyakawa, “Pin-on-disk wear behavior in a like-on-like configuration in a biological environment of high carbon cast and low carbon forged Co – 29Cr – 6Mo alloys,” *Acta Biomater.*, vol. 55, pp. 1309–1318, 2007.

[2] S. Sun, Y. Koizumi, S. Kurosu, Y. Li, H. Matsumoto, and A. Chiba, “Build direction dependence of microstructure and high-temperature tensile property of Co – Cr – Mo alloy fabricated by electron beam melting,” *Acta Mater.*, vol. 64, pp. 154–168, 2014.

[3] S. Sun, Y. Koizumi, S. Kurosu, Y. Li, and A. Chiba, “Phase and grain size inhomogeneity and their influences on creep behavior of Co – Cr – Mo alloy additive manufactured by electron beam melting,” *Acta Mater.*, vol. 86, pp. 305–318, 2015.

[4] J. Lugrin, N. Rosenblatt-Velin, R. Parapanov, and L. Liaudet, “The role of oxidative stress during inflammatory processes,” *Biol. Chem.*, vol. 395, no. 2, pp. 203–230, 2014.

[5] T. Lin *et al.*, “Chronic inflammation in biomaterial-induced periprosthetic osteolysis : NF- kB as a therapeutic target,” *Acta Biomater.*, vol. 10, no. 1, pp. 1–10, 2014.

[6] T. Dziubla and D. A. Butterfields, *Oxidative Stress and Biomaterials*. Academic Press, 2016, 2016.

[7] International Agency for Research on Cancer (IARC), “IARC MONOGRAPHS on the evaluation of carcinogenic risks to humans. Chromium, NIcckel and Welding,” Lyon, France, 1990.

[8] S. De Flora, M. Bagnasco, D. Serra, and P. Zanacchi, “Genotoxicity of chromium compounds. A review,” *Mutat. Res.*, vol. 238, pp. 99–172, 1990.

[9] S. De Flora, A. Camoirano, M. Bagnasco, and P. Zanacchi, *Chromium and carcinogenesis. Handbook of metal-ligand interactions in biological fluids. Bioinorganic Medicine*, Chromium a. New York, Marcel Dekker, 1995.

[10] S. De Flora, P. Zanacchi, and C. Bennicelli, *Toxicity of essential and beneficial ions. Handbook on Metal Ligand Interactions in Biological Fluids. Bioinorganic Medicine*, Toxicity o. New York, Marcel Dekker, 1995.

[11] S. De Flora, “Threshold mechanisms and site specificity in chromium (VI) carcinogenesis,” *Carcinogenesis*, vol. 21, no. 4, pp. 533–541, 2000.

[12] A. Oyane, H. Kim, T. Furuya, T. Kokubo, T. Miyazaki, and T. Nakamura, “Preparation and assessment of revised simulated body fluids,” *J. Biomed. Mater. Res. A*, vol. 65,

pp. 188–195, 2003.
[13] T. Takashima, Y. Koizumi, Y. Li, K. Yamanaka, T. Saito, and A. Chiba, "Effect of building position on phase distribution in Co-Cr-Mo alloy Additive Manufactured by Electron-Beam Melting * 1," *Mater. Trans.*, vol. 57, no. 12, pp. 2041–2047, 2016.
[14] A. H. Sun, Y. Koizumi, S. Kurosu, Y. P. Li, and A. Chiba, "Effect of phase transformation on tensile behavior of Co-Cr-Mo alloy fabricated by electron beam melting," *J. Jpn. Soc. Powder Powder Metall.*, vol. 61, no. 5, pp. 234–242, 2014.
[15] R. Rosenthal, B. R. Cardoso, I. S. Bott, R. P. R. Paranhos, and E. A. Carvalho, "Phase characterization in as-cast F-75 Co – Cr – Mo – C alloy," *J. Mater. Sci.*, vol. 45, pp. 4021–4028, 2010.
[16] J. V Giacchi, C. N. Morando, O. Fornaro, and H. A. Palacio, "Microstructural characterization of as-cast biocompatible Co – Cr – Mo alloys," *Mater. Charact.*, vol. 62, no. 1, pp. 53–61, 2010.
[17] J. V Giacchi, O. Fornaro, and H. Palacio, "Microstructural evolution during solution treatment of Co – Cr – Mo – C biocompatible alloys," *Mater. Charact.*, vol. 68, pp. 49–57, 2012.
[18] C. V. Vidal, A. I. Muniz, C. o. A. Olsson, and S. Mischler, "Passivation of a CoCrMo PVD alloy with biomedical composition under simulated physiological conditions studied by EQCM and XPS," *J. Electrochem. Soc.*, vol. 159, no. 5, pp. C233–C243, 2012.
[19] A. I. Muñoz and S. Mischler, "Interactive Effects of Albumin and Phosphate Ions on the Corrosion of CoCrMo Implant Alloy," pp. 562–570, 2007.
[20] C. V. Vidal and A. I. Muñoz, "Electrochemical characterisation of biomedical alloys for surgical implants in simulated body fluids," *Corros. Sci.*, vol. 50, pp. 1954–1961, 2008.
[21] E. Bettini, T. Eriksson, M. Boström, C. Leygraf, and J. Pan, "Influence of metal carbides on dissolution behavior of biomedical CoCrMo alloy : SEM , TEM and AFM studies," *Electrochim. Acta*, vol. 56, no. 25, pp. 9413–9419, 2011.
[22] E. Bettini, C. Leygraf, C. Lin, P. Liu, and J. Pan, "Influence of grain boundaries on dissolution behavior of a biomedical CoCrMo Alloy : In-situ Electrochemical-Optical , AFM and SEM / TEM Studies," *J. Electrochem. Soc.*, vol. 159, no. 9, pp. 422–427, 2012.
[23] C. V. Vidal and A. I. Munoz, "Effect of physico-chemical properties of simulated body fluids on the electrochemical behaviour of CoCrMo alloy," *Electrochim. Acta*, vol. 56, pp. 8239–8248, 2011.
[24] N. Sato and T. Ohtsuka, "Anodic oxidation of Cobalt in neutral and basic solution," *J. Electrochem. Soc.*, vol. 125, no. 11, pp. 1–6, 1976.
[25] L. . Burke, M. . Lyons, and O. . Murphy, "Formation of hydrous oxide ilms on cobalt under potential cyclic conditions," *J. Electroanal. Chem.*, vol. 132, pp. 247–261, 1982.
[26] V. Petr, *Electrochemical series in Handbook of Chemistry and Physics : 92nd Edition*. Chemical Rubber Company, 2011.
[27] R. Xu, X. Yang, P. Li, K. W. Suen, G. Wu, and P. K. Chu, "Eelectrochemical properties and corrosion resistance of carbon-ion-implanted magnesium," *Corros. Sci.*, vol. 82, pp. 173–179, 2014.
[28] D. Mareci, M. Romas, A. Cailean, and D. Sutiman, "Electrochemical studies of Cobalt-Chromium-Molybdenum alloys in artficial saliva," *Rev. Roum. Chim.*, vol. 56, no. 7, pp. 697–704, 2011.
[29] W. Jin, G. Wu, H. Feng, W. Wang, X. Zhang, and P. K. Chu, "Improvement of corrosion resistance and biocompatibility of rare-earth WE43 magnesium alloy by neodymium self-ion implantation," *Corros. Sci.*, vol. 94, pp. 142–155, 2015.
[30] G. Wu, Y. Liu, C. Liu, Q. Tang, X. Miao, and J. Lu, "Intermetallics novel multilayer structure design of metallic glass film deposited Mg alloy with superior mechanical properties and corrosion resistance," *Intermetallics*, vol. 62, pp. 22–26, 2015.

★★★